Progress in Organic Coatings 185 (2023) 107899

Contents lists available at ScienceDirect

Progress in Organic Coatings

journal homepage: www.elsevier.com/locate/porgcoat

Bio-based hybrid nanocomposites as multifunctional sustainable materials for stone conservation

P. Irizar [a,*], A. Pintor-Rial [b], I. Martinez-Arkarazo [a], M.A. Olazabal [a], L. Ruiz-Rubio [c,d], P. Cardiano [e], O. Gomez-Laserna [a]

[a] Department of Analytical Chemistry, University of the Basque Country (UPV/EHU), Barrio Sarriena s/n, E-48080 Leioa, Bizkaia, Spain
[b] Department of Biochemistry and Molecular Biology, University of the Basque Country (UPV/EHU), Barrio Sarriena s/n, E-48080 Leioa, Bizkaia, Spain
[c] Department of Physical Chemistry, University of the Basque Country (UPV/EHU), Barrio Sarriena s/n, E-48080 Leioa, Bizkaia, Spain
[d] BCMaterials, Basque Center for Materials, Applications and Nanostructures, UPV/EHU Science Park, 48940 Leioa, Spain
[e] Department of Chemical, Biological, Pharmaceutical and Environmental Sciences, University of Messina, Viale F. Stagno d'Alcontres 31, I-98166 Messina, Italy

ARTICLE INFO

Keywords:
Epoxy-silica hybrids
Ionic liquids
Nanotechnology
Biocides
Artificial ageing test
Stone conservation

ABSTRACT

This study was aimed at developing a sustainable versatile bio-based epoxy-silica material to be potentially employed as hydrophobic and biocidal consolidating product in the field of stone conservation. For this purpose, two hybrid formulations containing 2,2,4,4-tetramethyl-1,3-cyclobutanediol diglycidylether (CBDO-DGE), a cycloaliphatic epoxy precursor derived from the arnica root, together with (3-glycidyloxypropyl)trimethoxysilane (GPTMS) and octyltriethoxysilane (OcTES) as silica-forming additives, were chosen as the basis of the multifunctional material to be finely adjusted and gain biocidal properties. With this goal in mind, different synthetic strategies based on ionic liquids (ILs), essential oils (EOs) and nanoparticles (NPs) doping have been employed. Specifically, dimethyloctadecyl[3(trimethoxysilyl)propyl]ammonium chloride (QAS), tetradecyl phosphonium chloride (QPS) and thymol, as well as cerium-TiO_2 NPs and thymol-loaded SiO_2 NPs were incorporated into the starting hybrid formulations, during the sol-gel process, to investigate their influence on the network formation. First, distribution studies by scanning electron microscopy/energy-dispersive X-ray (SEM-EDS) analysis were performed, whereas the suitability of each formulation to match the main requirements for a stone conservation material was evaluated in terms of thermostability, hydrophobicity and inhibition of the microbiological growth by a combination of TG-DTA, DSC, dynamic mechanical analysis (DMA), with contact angle and disk-diffusion measurements, respectively. Based on the data analysis, it was observed that the direct incorporation of ILs and EOs had an adverse effect on the ability of GPTMS to act as a coupling agent. This resulted in decreased thermal stability and a 50 % reduction in glass transition temperatures, along with the retention of hydrophilic behavior. In contrast, the inclusion of NPs did not significantly interfere with the hybrid network formation, and effectively maintained the thermo-mechanical and hydrophobic properties of the hybrids within satisfactory parameters. Consequently, both nanocomposite materials were further tested on stone samples by artificial ageing experiments under acidic atmosphere. In view of the results, the hybrid enriched with thymol-loaded SiO_2 NPs demonstrate the most suitable thermo-mechanical and hydrophobic properties (T_{onset}, T_α and CA values of 276 °C, 54 °C and 100°, respectively), as well as a proper biocidal capability against bacteria. Furthermore, the developed material provided effective stone protection, resulting in a 92 % reduction in material loss, while preserving the substrate chromatic characteristics (ΔE 2.23). These findings suggest that the proposed treatment meets the first main requirements for stone conservation.

1. Introduction

In recent years, research endeavors have predominantly concentrated of identifying sustainable alternatives to fossil resources that exhibit industrial feasibility to cover a wide range of applications and areas. In this context, while the preservation of stone building materials has emerged as a significant multidisciplinary research field fostering economic and cultural growth [1,2], viable environmentally-friendly

* Corresponding author.
E-mail address: Pablo.irizar@ehu.eus (P. Irizar).

https://doi.org/10.1016/j.porgcoat.2023.107899
Received 29 May 2023; Received in revised form 9 August 2023; Accepted 18 August 2023
Available online 23 August 2023

alternatives have not been thoroughly explored within the building and restoration sectors. Consequently, the utilization of consolidating and coating products derived from epoxy compounds of Bisphenol A (BPA) remains prevalent for treating extensive lithic surfaces [3]. In addition, cleaning and preventive protocols often rely on the use of harmful biocides and antifoulants, which also have adverse implications for the Sustainable Development Goals (SDGs) [4,5]. Biocidal active compounds are designed to affect living organisms, but their impact is not limited to targeted harmful organisms, as the non-target organisms can also be harmed when these substances enter their habitats. Furthermore, humans can potentially be affected during product use or when exposed to treated materials if proper handling is not followed. Consequently, growing societal awareness demands novel effective solutions that go beyond decisions based solely on cost-effectiveness and short-term outcomes. Instead, it is crucial to consider environmental aspects, prioritize the health of personnel involved, and emphasize responsible production as significant factors requiring industrial attention.

In this respect, innovation in stone treatment should encompass consolidation requirements, while offering additional protection against the detrimental effects of water and biodeterioration agents [6,7]. Therefore, the desired range of capabilities for a stone conservation product necessitates the specific development of advanced trifunctional materials that guarantee the use of minimal amounts of toxic compounds.

As a starting point, research on bio-based renewable epoxy precursors offers the potential to strongly reduce the production and consumption of BPA, thereby enabling industry and society to embrace environmentally friendly solutions and evolve within sustainable technologies. Once bio-based thermosets are selected, various strategies can be used to exploit their potential as organic foundations for the development of advanced materials for stone conservation purposes [8,9]. Specifically, bio-based epoxy-silica hybrids have proven their effectiveness in the field as highly promising coatings and consolidating products [10–13]. Generally speaking, the incorporation of organic and inorganic phases into a hybrid matrix leads to the combination of different features, thus allowing to achieve with ease improved and/or additional properties with respect to the parent counterparts, which can be further tailored to fit specific functions [14,15]. This means that by utilizing a variety of synthetic approaches, often under mild conditions, the proper selection of starting compounds and their relative ratios can be specifically adapted to build composite materials that meet suitable thermal and mechanical characteristics, display a stone-compatible chemistry, having the ability to recover and maintain its integrity against the effects of outdoor exposure, while reducing the penetration of water into the lithic substrates without causing surface aesthetic alterations [16].

In this respect, 2,2,4,4-tetramethyl-1,3-cyclobutanediol diglycidyl ether (CBDO-DGE) has recently been highlighted as building block for the development of epoxy-silica networks for stone conservation purposes. It is a low molecular weight bioepoxy resin, derived from arnica root [10,17]. CBDO-DGE formulations developed from triethylenetetramine (TETA), in the presence of octyltriethoxysilane (OcTES) and/or (3-glycidyloxypropyl)trimethoxysilane (GPTMS) as silica forming additives (Fig. S1), have shown promising properties as consolidating and hydrophobic smart materials, being transparent with light yellowish tone, with a thermal resistance up to 437 °C, a glass transition temperature (T_α) of 55.8 °C and contact angles (CA) that reached values of 105°. To achieve multifunctional hybrid materials, various strategies can be employed to incorporate additional biocidal properties into the base conservation products. Among the most widely used, doping with ionic liquids (ILs) and nanoparticles (NPs) has been shown to allow the fine modulation and/or to introduce extra capabilities into the resulting material, including biocidal properties [18–20]. As for the incorporation of ILs during hybrid synthesis, depending on the IL structure, it could act as a catalyst for sol-gel process, as a molding agent to improve the quality of inorganic domains and/or as coupling agent to decrease interfacial tensions between the silica filler and the organic matrix, while imparting other properties to the final material [21–24]. Through the proper selection of cations and anions, several challenging applications have been explored, being widely exploited in the field of cultural heritage as biocidal cleaning treatments, and lastly as corrosion inhibitors, to preserve metallic artifacts and old paper documents, among others [25–32]. Possible options include quaternary ammonium (QASs) and phosphonium salts (QPSs) as active compounds against bacteria, fungi, parasites, and even lipophilic viruses. Consequently, while their incorporation in an epoxy-silica hybrid is expected to impart biocidal capabilities to the material, depending on their functional groups and on the length of the aliphatic chains, they could contribute to the cross-linking or remain dispersed in the matrix, thus balancing the main features of the starting epoxy hybrid in terms, for instance, of enhanced hydrophobicity [33–35].

For the above purpose, even greener alternative may be the incorporation of essential oils (EOs), such as eugenol, carvacrol, thymol, menthol, and so on, which have shown remarkable biocidal activity due to the presence of phenols, aldehydes and alcohols, and also a suitable miscibility with consolidating formulations [21,36–38]. In principle, thanks to their functional groups, EOs could take part to the development of the hybrid system. Alternatively, they could be only dispersed in the hybrid network, thus altering the base material, with a negative impact on its main properties. In addition, EOs high volatility and degradation rate are disadvantages to be considered in the material design [39,40]. At this respect, the benefits provided by nanotechnology could offer a solution by using mesoporous silica NPs or halloysite nanotubes that allow EOs pre-encapsulation [41,42]. In fact, NPs have been widely exploited in stone conservation treatments due to their hydrophobic, consolidating, biocidal and/or self-cleaning capabilities, *i.e.* metal NPs (Au, Ag, Pt), oxides and hydroxides NPs (TiO_2, SiO_2, ZnO, $Ca(OH)_2$, $Mg(OH)_2$, $Sr(OH)_2$), or even hydroxyapatite and carbonated derivatives [16,43–45]. However, the highest potential of nanotechnology usually comes from the design of nanocomposite materials. These materials have the ability to act as reinforcing agents improving hydrophobic and thermo-mechanical properties. Additionally, they can incorporate biocidal capabilities, enabling the development of advanced tailor-made products for different stone lithotypes and protection needs [46,47]. Specifically, TiO_2 and lanthanide-TiO_2 NPs have demonstrated their high effectiveness when combined with silane/siloxane and acrylic or epoxy matrices. This combination enhances hydrophobicity, thermal resistance and photocatalytic activity [22,23,48,49]. Furthermore, SiO_2 NPs have also showed their ability to enhance conventional consolidating formulations based on alkoxysilane compounds, resulting in superhydrophobic properties. Simultaneously, they provide protection against ultraviolet radiation degradation [50–52].

According to this, and aligned with sustainability values, the primary objective of the work addressed here is to develop a specific tailored material for stone conservation that exhibits the desired trifunctionality, maintaining a suitable balance among hydrophobic, consolidation and biocidal properties.

Regarding to the previous studies focused on synthesis and characterization of CBDO-DGE hybrids [10], GPTMS based formulation were pointed out as a highly cross-linked and slightly rigid network with the potential to be modulated by a plasticizing effect exerted by the incorporation of the long aliphatic ILs chains or EOs. Thus, dimethyloctadecyl [3(trimethoxysilyl)propyl] ammonium chloride (QAS), trihexyl(tetradecyl)phosphonium chloride (QPS) and thymol were studied as network additives for the properties fine tuning as well as to introduce biocidal capabilities [53–55]. As for NPs addition, the opposite effect could be theoretically predicted, expecting to act as a reinforced load of the epoxy-silica network [56], so the formulation based on GPTMS and OcTES that have previously shown higher flexibility was selected for this kind of doping strategy. Specifically, cerium-doped TiO_2 NPs with proven capabilities to improve coating hydrophobicity, and impart significant self-cleaning and biocidal activity to epoxy-silica hybrids

similar to the ones here reported, were synthetized and tested as nanofiller [6]. In addition, to reduce the volatility of thymol and avoid the possible detriment of the hybrid network properties, while maintaining biocidal potential activity, a parallel approach based on the encapsulation of thymol into mesoporous SiO_2 NPs was also here explored. Among the variety of functions that ILs, EOs and NPs can offer in the development of hybrid materials, investigating their interaction and distribution within the epoxy-silica network can lead to a better understanding of the advantages and limitations associated with their use in a specific material system. This research provides valuable information for predicting their impact on thermo-mechanical and hydrophobic properties of the material. It also explores the potential to obtain advanced multifunctional materials with biocidal capability, which could be applicable to a wide range of fields.

2. Material and methods

2.1. Materials and reagents

All the chemicals used, namely 2,2,4,4-tetramethyl-1,3-cyclobutanediol (≥99 %) (CBDO), epichlorohydrin (≥99.0 %) (ECH), tetra-n-butylammonium bisulfate (≥99 %) (TBAB), triethylenetetramine (≥97 %) (TETA), octyltriethoxysilane (≥97 %) (OcTES), tetraethoxysilane (≥97 %) (TEOS), (3-glycidyloxypropyl)trimethoxysilane (≥97 %) (GPTMS), dimethyloctadecyl[3(trimethoxysilyl)propyl]ammonium chloride (≥97 %) (QAS), tetradecyl phosphonium chloride (≥95 %) (QPS), thymol, titanium isopropoxide (≥97 %) (TTIP) and cerium nitrate hexahydrated (≥99 %), were purchased from MERCK and used as received.

2.2. Synthetic procedures

2.2.1. Synthesis of 2,2,4,4-tetramethyl-1,3-cyclobutanediol diglycidyl ether (CBDO-DGE)

The CBDO-DGE was synthesized according to the procedures reported [10,15]. Briefly, CBDO (2.8 g) and ECH (15.5 mL) were reacted, adding TBAB (0.65 g) as phase transfer catalyst, sodium hydroxide (7.5 g) and few drops of Milli-Q water. The mixture was left under stirring for 2 h at 40 °C and then allowed to reach room temperature. The crude was recovered using dichloromethane, washed with a mixture of Milli-Q water and acetic acid, and then dried over anhydrous sodium sulfate. Finally, the solvent was removed by vacuum. The CBDO-DGE monomer was obtained as a pale-yellow liquid with an epoxy equivalent weight (EEW) of 128.17 g eq^{-1} and an epoxide value of 7.80 eq Kg^{-1}. Yield = 68 %.

2.2.2. Synthesis of NPs: thymol-SiO_2 and Ce-doped TiO_2

The synthesis of thymol-SiO_2 mesoporous NPs was carried out by mixing TEOS (380 μL), ethanol (12 mL), an aqueous solution of thymol (60 μL, 10 % m/v) and ammonium hydroxide (1 mL, 26 % m/v). The reaction mixture was stirred for 48 h at room temperature. The resulting NPs were then separated by centrifugation (30 min at 10,000 rpm), washed with ethanol and dried at room temperature for one day [41]. The expected product was obtained as a white fine powder.

Titania nanoparticles were synthesized by mixing titanium isopropoxide (0.5 g) with isopropanol at a ratio of 1:30. Once the colloidal suspension was formed, cerium nitrate hexahydrate (0.023 g) was added (0.03:1 ratio, with respect to TTIP) and stirred for 1 h. Then, the NPs were washed and centrifuged three times, using isopropanol, ultrapure water and ethanol, respectively [6]. The solid was left at 80 °C for 48 h and then thermally cured at 450 °C for 3 h, with a heating rate of 2 °C min^{-1}, to gain a pale-yellow solid, namely Ce^{3+}-TiO_2 in anatase polymorph form.

2.2.3. Synthesis of the CBDO-DGE doped multifunctional hybrids

Two different organic-inorganic hybrid formulations, namely CBDO-DGE/GPTMS and CBDO-DGE/GPTMS/OcTES, were doped with selected additives able to add biocidal properties without compromising consolidating and hydrophobic features already displayed by the base hybrids [10]. Specifically, samples 1–3 were obtained using ILs and EOs as dopants. Briefly, three mixtures containing CBDO-DGE (0.25 g), GPTMS (0.25 g) and MeOH (8 mL) were left on stirring for 60 min at room temperature. Then, a stoichiometric ratio of TETA amine required to react with CBDO-DGE and GPTMS oxiranes was added to each mixture and, after 30 min of reaction, QAS, QPS or thymol were added in a 3 % w/w fixed amount to gain 1, 2 and 3 samples, respectively (Table 1). The reaction mixtures so obtained were further stirred for 90 min. For samples 4 and 5, NPs and thymol-loaded NPs were used as nanofillers. In detail, two aliquots of CBDO-DGE (0.30 g), GPTMS (0.20 g) and methanol (4 mL) were reacted for 60 min at room temperature. Then, after the proper amount of TETA was added, TiO_2-Ce^{3+} NPs and thymol-loaded SiO_2 NPs were incorporated into the mixtures at 3 % w/w to obtain 4 and 5 samples, respectively. Pre-hydrolyzed OcTES (0.025 g) was then added to each mixture by a dropping funnel, and the suspensions left under stirring for 90 min (Table 1). The reaction mixtures (1–5) were transferred into 5 cm diameter Teflon Petri dishes and left on standing for 4 days, to allow the solvent evaporation. The films obtained were thermally cured at 60 °C for 24 h, reached at a heating rate of 5 °C min^{-1} [10].

2.3. Biocidal capacity tests

Biocidal properties of the doped hybrid formulations were investigated by disk-diffusion method experiments. The films were cut into 10 mm diameter disks, dried at 60 °C in a vacuum oven ($<10^{-2}$ Torr) for 24 h, and subsequently sterilized by immersion in 70 % ethanol for 10 min. Then, under aseptic conditions, tryptone soy agar (TSA) plates were inoculated with 100 μL of a freshly prepared *Arthrobacter spp.* [57,58] suspension of approximately 1.5 × 108 CFU mL^{-1} and spread over the entire agar surface using a sterile cotton swab. After the disks were placed on agar surface, the plates were aerobically incubated at 25 °C for 48 h under visible irradiation [57]. The antimicrobial halo (n_{whalo}) was calculated according to the equation: $n_{whalo} = \frac{\left(\frac{d_{iz}-d}{2}\right)}{d}$, where d_{iz} is the inhibition zone and d the disk diameter [59].

2.4. Stone specimens tests

A natural Mediterranean calcarenite was chosen for stone testing due to its widespread presence in the Mediterranean Basin since the Bronze Age. This lithotype can be found in countries such as Spain, Portugal, Italy, Greece, Tunisia, and others. This type of stone is extracted from numerous quarries across Europe, and specifically, the *Albamiel* variety used in this study (apparent density of 1.940 Kg m^{-3}, porosity of 28.2 % and water absorption capacity of 14.53 %) was sourced from the representative Rosales quarry (Albacete, Spain). Slabs of this stone were purchased from the Rosal Stones Company (Murcia, Spain). This Mediterranean calcarenite has historical significance in Iberian culture. It

Table 1
Relative amounts of the reactants employed for the syntheses of the doped CBDO-DGE epoxy-silica resins.

Sample name	CBDO-DGE	GPTMS	OcTES	Additive 3 % w/w
1	0.25 g 0.98 mmol	0.25 g 1.06 mmol	–	QAS
2	0.25 g 0.98 mmol	0.25 g 1.06 mmol	–	QPS
3	0.25 g 0.98 mmol	0.25 g 1.06 mmol	–	thymol
4	0.30 g 1.17 mmol	0.20 g 0.85 mmol	0.025 g 0.09 mmol	TiO_2 + Ce^{3+}
5	0.30 g 1.17 mmol	0.20 g 0.85 mmol	0.025 g 0.09 mmol	SiO_2 + thymol

gained popularity during the Roman Empire through the *Cartago Nova* trade route, spreading its usage throughout the Iberian Peninsula and northern Europe. As a result, it was employed by various cultures for a wide range of applications, including fortifications, bridges, aqueducts, temples, and religious sculptures. Notable examples of its use can be found in the *Lady of Offering*, *Tolmo de Minateda*, and the *Alhambra*. Even today, it is extensively employed in its region of origin for the construction of external facades and pavements. Additionally, it plays a crucial role in the restoration of heritage buildings [50,60–62]. To conduct the study, standard stone specimens were obtained by cutting larger samples into 2 × 2 × 2 cm cubes [63]. The samples were then weighed and investigated by colorimetry. The selected formulations were slowly applied by cycles of impregnation method to cover all the cube faces; then the treated stones were introduced into a desiccator under vacuum to allow the products to reach in the inner parts of the samples [64,65]. Then, each stone specimen was left at room temperature for 4 days to ensure the evaporation of the solvent, cured at 60 °C for 24 h and weighted to check for mass variation. Consequently, 3 replicates per selected formulation, plus 3 untreated stone specimens, used as reference, were artificially aged for one month under a CO_2 atmosphere at 50 °C and humidity up to saturation (based on UNE-EN 13919). The effects of artificial ageing were at first evaluated by colorimetric investigations and Scotch peeling tests on stone surfaces, as well as mass loss measurements [66]. Finally, surface analysis of stone specimens was performed using optical image and Scanning Electron Microscope (SEM) imaging analysis for comparison purposes.

2.5. Instruments

Attenuated total reflection Fourier transform infrared spectroscopy (ATR-FTIR) measurements were collected by a Jasco 6300 spectrophotometer with a PIKE MiracleTH module. The equipment consists of a Ge/KBr beam splitter, and a deuterated L-alanine doped triglycene sulphate (DLATGS) detector with Peltier temperature control. All the spectra were recorded in the middle infrared region, namely from 4000 to 400 cm^{-1}, accumulating 220 scans, with a spectral resolution of 4 cm^{-1}. Data acquisition was performed by means of a Jasco Spectra Manager Suit package, while Origin 2018 program was employed for the data treatment.

X-ray powder diffraction (XRD) analyses were carried out by means of a Bruker D2 Phaser desktop diffractometer, with a Cu tube (λ = 1.54056 Å), recording the data in the 2θ range of 20–90° with an angular step size of 0.025°. Diffractograms were analyzed using the International Centre for Diffraction Data (ICDD) database.

The dual M4 TORNADO ED-XRF spectrometer (Bruker Nano GmbH, Berlin, Germany) with a micro-focus Rh X-ray tube (50 kV and 600 μA) connected to a poly-capillary system that allows to work under a lateral/spatial resolution of 25 μm measured for Mo Kα (around 17 mm at 2.3 keV to 32 μm at 18.3 keV) was employed. The detection of the fluorescence radiation was performed using an XFlash® silicon drift detector with 30 mm^2 of the sensitive area and an energy resolution of 145 eV for Mn-Kα. The selected line for the elements detection was the Kα1 and the live time employed for each single acquisition was 150 s. In addition, to improve the detection capability, the measurements were acquired under vacuum (20 mbar) by means of a diaphragm pump MV 10 N VARIO-B. Data collection and interpretation were carried out by means of the M4 TORNADO (Bruker Nano GmbH) software.

Transmission Electronic Microscopy (TEM) analyses were carried out by a TECNAI G2 20 TWIN equipment (200 kV and LaB6 filament). The NPs samples were prepared by dispersion into methanol in an ultrasonic bath for 15 min, and spread onto a copper grid (300 Mesh) covered by a carbon film followed by vacuum drying.

SEM-EDS analysis was carried out by an EVO®40 Scanning Electron Microscope (Carl Zeiss NTS GmbH) coupled to an X-Max Energy-Dispersive X-Ray spectrometer (Oxford Instruments). The film and stone samples analyzed were vacuum sputtered with 10 nm gold particles (<20 μm), to improve the signals in an Emitech K550X sputter coater vacuum chamber (Quorum Technologies LTD). Secondary electron (SE) images were acquired at high vacuum employing an acceleration voltage of 20 kV. The elemental mapping analyses were performed using a 10 mm working distance, a 35° take-off angle, and a 20 kV acceleration voltage. The data were processed with INCA Microanalysis Suite software v 4.3 (Oxford Instruments).

A RoHS X4 digital microscope with a focus range of 15–40 mm was used for the optical microscopic stone visual inspection. The images were obtained and processed using HiView 1.4.

TGA data were acquired by a TA Instruments Q500 thermal analyzer, under nitrogen flow of 10 mL min^{-1}, in the temperature range between 25 °C and 800 °C with a heating rate of 10 °C min^{-1}. DSC experiments were carried out with a Mettler Toledo DSC3+, in the temperature range between −60 and 220 °C, at a heating rate of 10 °C min^{-1}, under a nitrogen flow of 20 mL min^{-1}. DMA measurements were acquired by an analyzer Epexor 100 N GABO Qualimeter on rectangular specimens of 8.0 mm × 12.0 mm × 2.9 mm, in a temperature range from −70 to 150 °C, at a heating rate of 2 °C min^{-1} in tension mode. The tests were carried out at a strain rate of 0.5 % and 0.2 % for Static and Dynamic, respectively. DSC, TGA and DMA data were processed using Excel software v 2017.

Contact angle (CA) investigations were performed by means of the Neurtek Instruments Dataphysics OCA 15EC system. Milli-Q water drops (2 μL $drop^{-1}$) were deposited onto the samples surface and the average of 5 measurements was reported.

A PCE-CSM 5 colorimeter (PCE Instruments), equipped with a silicon photoelectric diode sensor, was employed to obtain the L*a*b* color space average values (ASTM D-1925, CIE 1976) of the hybrid film surface. The instrument was calibrated on a standard white cap reference before each measurement, then the data were acquired according to the NORMAL Protocol 43/93 [67].

Atmospheric ageing tests were carried out using an Autonics Kesternich chamber equipped with a TK4S High Accuracy PID control module, using as experimental parameters 50 °C and humidity up to saturation and 2 L of CO_2 as the precursor of the acidic atmosphere.

3. Results and discussion

3.1. NPs characterization: thymol-SiO_2 and Ce-doped TiO_2

The successful synthesis of SiO_2 NPs was confirmed by XRD diffractograms displaying the characteristic signal at 23.2° 2θ, and further corroborated by the presence of the bands at 1097, 957 and 799 cm^{-1} in the infrared spectrum, which were attributed to the Si—O—Si asymmetric stretching, Si—OH stretching, and Si—O—Si symmetric stretching vibrations, respectively [11]. The absence of the peak at 1634 cm^{-1}, commonly attributed to O—H bending vibration mode of physisorbed water molecules inside the pores, suggested that the pores, very likely, being water-free, were filled with thymol. This assumption was further ascertained by means of biocidal tests (see later). Besides, the —OH groups of the Si—OH moieties on SiO_2 NPs surface were assigned to the broad band at 3445 cm^{-1}. In the case of Ce-doped TiO_2 NPs, diffractograms revealed peaks at 25.6, 38.2, 48.3, 54.2, 55.4, 62.8, 69.1, 70.3, and 75.3° 2θ, evidencing the occurrence of anatase as major phase (>98 %), *i.e.* the TiO_2 polymorph with biocidal properties [68]. The presence of Cerium was roughly confirmed by the quite low spectral signal/noise ratio obtained in the diffractogram, as already observed [6,7]. However, the Ce^{3+} inclusion was finally corroborated by XRF data that showed its characteristic signals at 34,719.7 eV (Ce K_α).

TEM analysis showed the average size of the thymol-SiO_2 and Ce-doped TiO_2 NPs around 100 nm and 200 nm, respectively (Fig. 1).

3.2. Characterization of CBDO-DGE doped multifunctional hybrids

In order to incorporate biocidal activity into the epoxy-silica

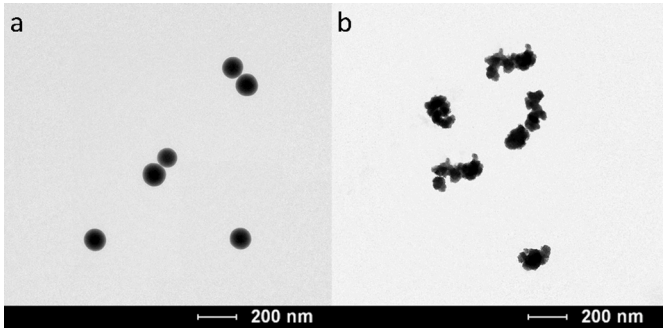

Fig. 1. Transmission Electronic Microscope (TEM) images: a) Mesoporous thymol-loaded SiO_2 NPs and b) Ce-doped TiO_2 NPs.

products, preserving, as much as possible, their thermo-mechanical and hydrophobic characteristics, several doping tests were carried out. More in detail, prior to carry out biocidal activity tests, materials based on CBDO-DGE/GPTMS and CBDO-DGE/GPTMS/OcTES were doped with selected additives and investigated to verify if the proper balance of the consolidating and hydrophobic features already shown by the base hybrids was maintained.

From the visual inspection, 1–3 samples, *i.e.* those doped with ILs and EO, appeared slightly more flexible than the corresponding non-doped ones, without any significant chromatic alteration. As expected, 4 and 5 samples gained a harder texture upon NPs doping. In addition, Ce-doped TiO_2 NPs imparted a light-yellow coloration to the lower part of the film, probably as a consequence of their deposition during the solvent evaporation process, whereas no macroscopic color variation occurred by the implementation of thymol-SiO_2 NPs, suggesting a homogeneous distribution into the hybrid film.

The effect of doping in the formation of the hybrid networks was firstly investigated by secondary electron images (SE) and elemental distribution mappings. Previous studies on CBDO-DGE hybrids [10] evidenced that the use of GPTMS as the sole silica precursor leads to the formation of a homogeneous and highly crosslinked epoxy-silica network. Here, the analysis of SE images collected for samples 1, 2, and 3 (Fig. 2) indicated that quite homogeneous silicon distribution was obtained, evidencing that QAS, QPS and thymol were dispersed into the hybrid matrix; at the same time, small micro-phase separation areas (<10 μm) were detected in all cases suggesting that the doping with ILs and EO exerted a negative impact on the GPTMS capability to act as coupling agent. This last phenomenon was more prominent in QAS and thymol formulations probably due to the self-condensation processes that may prevail during the sol-gel reaction for silanol and hydroxyl groups coming from additives, over the co-condensation with OH-formed upon GPTMS hydrolysis [10,69]. On the other hand, the proper combination of GPTMS and OcTES for CBDO-DGE hybrids development was demonstrated to be a successful approach to get a balanced set of thermal and mechanical properties thanks to the double role exerted by OcTES [10], which was capable to act as plasticizer at low ratios and, at the same time, it could provide some anchor points during the formation of the organic-inorganic network. At this respect, the SE images of the nano-enriched sample 4 (Fig. 2) revealed that the addition of TiO_2-Ce caused the formation of surface pores with sizes in the range of 20–60 μm. The silicon distribution in the mapping was homogeneous so that, apparently, well-crosslinked hybrid networks were formed without any observable phase separation phenomena. However, in titanium mapping aggregates can be observed. This evidence suggested that TiO_2-Ce NPs, being not able to participate to the development of the hybrid system, could only act as a filler. Conversely, in the case of sample 5, containing thymol-SiO_2 NPs, a completely smooth surface was observed probably due to their theoretical ability to promote crosslinking with GPTMS during the sol-gel reaction thanks to the active hydroxyl groups moieties available on the silica surface. This finding clearly indicated

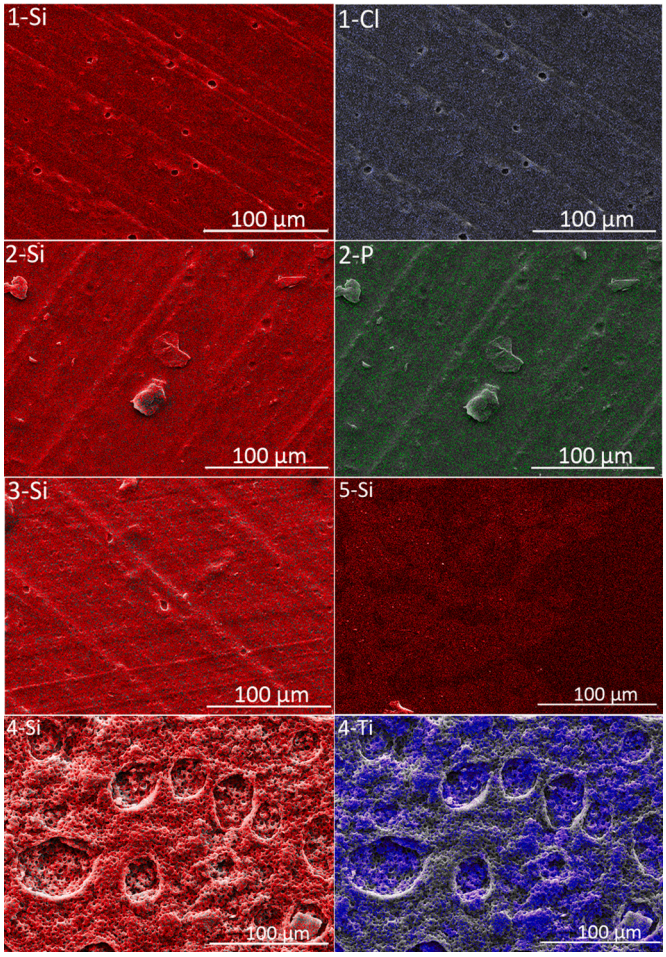

Fig. 2. SEM-EDS images of 1–5 hybrid samples. Samples 1–3 were formulated from GPTMS as silica precursor, and doped with QAs, QPs and thymol, respectively; 4–5 from GPTMS and OCTES as silica precursors, and nano-reinforced with Ce-TiO_2 and thymol-SiO_2 NPs, respectively. Silicon, chlorine, phosphorous and titanium distribution mappings are overlayed, in red, dark blue, green and light blue color, on the SE images acquired at a magnification of 1000×. (For interpretation of the references to color in this figure legend, the reader is referred to the web version of this article.)

that the addition of thymol-SiO_2 NPs allowed the formation of a tight and homogeneous epoxy-silica network and, depending on the interaction that the enhanced silica network may have had with the OcTES silica precursor, an improvement of hydrophobic and thermal properties could result.

At this respect, studies on thermal behavior of samples 1–5 were carried out by TGA analysis (Table 2, Fig. S2). Accordingly, samples 1, 2, 4, and 5 showed thermal degradation under nitrogen atmosphere

Table 2
Thermal data of the 1–5 doped hybrid samples.

Samples	1	2	3	4	5
First step					
T_{onset} [°C]	270	259	305	253	276
T_{max} [°C]	333	335	336	340	331
% mass loss	67.6	58.0	95.1	57.2	54.2
Second step					
T_{onset} [°C]	407	442		410	396
T_{max} [°C]	452	463		431	435
% mass loss	17.8	20.8		21.3	25.9
% residual mass[a]	14.6	21.2	4.9	21.5	19.9
T_g [°C]	24.4	19.9	20.2	36.6	31.0

[a] At 800 °C.

occurring in two steps ending below 600 °C. On the contrary, the thymol containing sample 3 displayed a single degradation step characterized by T_{onset} and T_{max} values of 305 and 336 °C, respectively, and a very high mass loss (95.1 %) occurring at a relative low temperature. Although the residue mass observed for this sample was very low, in contrast with all the others (*i.e.* between 14.6 and 21.5 %), an increased resistance upon heating with respect to the corresponding undoped hybrid (whose T_{onset} was 273 °C) was detected. Conversely, comparable or lower thermal stability were observed for ILs doped samples 1 and 2 (*i.e.* T_{onset} of 270 and 259 °C, respectively), with respect to 273 °C achieved by the original formulation. Higher T_{onset} values were gained for the second thermal event, with 407 and 442 °C for sample 1 and 2, respectively, with respect to 394 °C found for the ILs-free hybrid. As far as residual mass values are concerned, 14.6 and 21.2 % for 1 and 2 samples were observed, whereas for non-doped formulation it was 22.5 % [10]. As for samples 4 and 5 thermal stability generally decreased, showing T_{onset} values of 253 and 276 °C, *versus* 290 °C of the undoped hybrid, whereas residual masses found at the end of thermogravimetric scannings were comparable, *i.e.* 21.5 and 19.9 %, respectively, *versus* 18.8 °C for starting hybrid [10]. These results evidenced that the thymol incorporation in the mesoporous SiO_2 NPs could be a successful strategy to provide biocidal capability to the hybrids without modifying to a great extent the base network requirements previously obtained using GPTMS and OcTES as silica forming additives.

The DSC thermograms (Table 2) showed glass transition temperatures (T_g) values reduced more than a half for samples 1, 2, and 3 of 24.4, 19.9 and 20.2 °C respect to the 48.4 °C achieved by the non-doped hybrid [10]. These findings clearly indicated that the GPTMS capability to act as coupling agent was strongly affected by the presence of ILs and EO so that a significant decrease of the cross-linking degree in the resulting hybrids may occur [70]. Although, in principle, SiOMe groups of QAS, after hydrolysis, could actively concur to the condensation of silanols coming from GPTMS thus providing additional anchor points for the hybrid development, the rather low T_g obtained for sample 1 suggested that the plasticizing effect due to the alkyl chains of QAS actually prevailed over the cross-linking with GPTMS so that the efficient incorporation of QAS into the hybrid network seemed unlikely.

By contrast, for samples 4 and 5, the detected T_g were slightly lower (*i.e.* values of 36.6 and 31.0 °C, respectively) than the one (39.1 °C) observed of the non-doped sample [10], evidencing that the use of thymol-containing NPs, rather than neat thymol, could be a successful strategy to provide EO biocidal properties to the products without a strong negative impact on the hybrid development.

The DMA investigations (Table 3 and Fig. 3) displayed for sample 1 a T_α value of 36.3 °C, close to the T_g, thus suggesting that QAS may actively concur to the development of organic-inorganic network, although not to a great extent. Again, from the data collected, it can be noticed that the use of QPS and thymol as additives in samples 2 and 3 resulted in a clear plasticizing effect, as the difference between T_g and T_α values was in both cases around 20 °C, with T_α of 39.7, and 39.1 °C, respectively. In contrast, the loading of hybrids with NPs, as for samples 4 and 5, provided T_α of 44 and 54 °C, respectively, thus confirming that their incorporation actually preserved the cross-linking degree. This was even more evident for 5 sample, suggesting that an efficient incorporation of NPs in the hybrid matrix occurred very likely due to the co-condensation of silica OH- groups with the silanols coming from the alkylalkoxysilanes, without compromising the intrinsic flexibility of the non-doped original formulation.

Table 3
Dynamic-mechanical properties of the 1–5 doped hybrid samples.

Samples	1	2	3	4	5
E′ (25 °C) [MPa]	426.6	450.5	559.0	731.2	923.2
E″ (25 °C) [MPa]	155.76	133.73	170.44	151.95	128.69
T_α [°C]	36.3	39.7	39.1	44.0	54.0

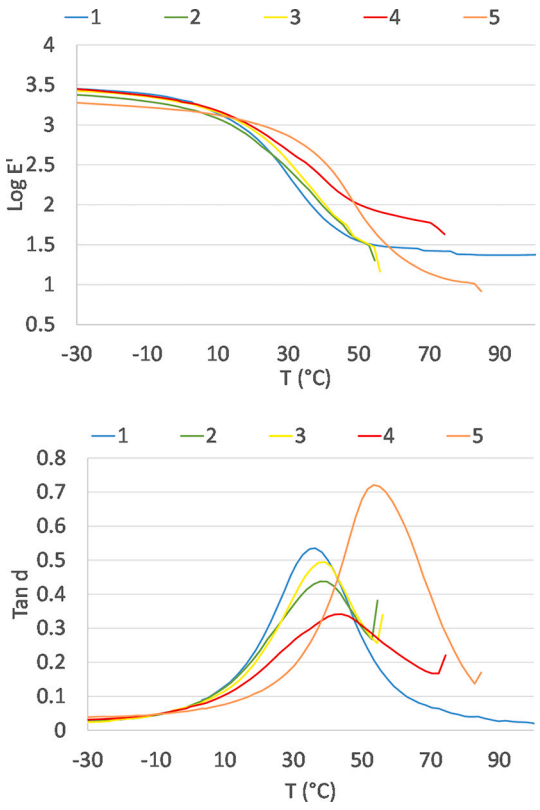

Fig. 3. Log storage modulus (E′) and damping (tan δ) of 1–5 hybrid samples as a function of temperature.

The hydrophobic behavior of samples 1–5 was assessed by contact angle measurements. The collected contact angle average data are displayed in Fig. 4, where two groups can be clearly distinguished. Samples 1, 2 and 3 showed contact angle values lower than 90°, thus indicating that the purpose of improving the hydrophobic capacity of the original hybrid by the incorporation of ILs or neat thymol was not achieved. On the contrary, the nano-enrichment with thymol-SiO_2 NPs preserved the original hydrophobic capability, with a CA value of 100°. However, the most significant result was obtained for sample 4, where the enrichment of the formulation with Ce-doped TiO_2 NPs imparted an increase of 12° in the hydrophobicity, with respect to the undoped hybrid [71].

From the whole of the collected data, it clearly appeared that nano-enriched hybrid samples 4 and 5 are the ones that displayed thermo-mechanical and hydrophobic properties suitable for stone conservation purposes. Accordingly, further studies were carried out to determine the biocidal capability and validate their multifunctional

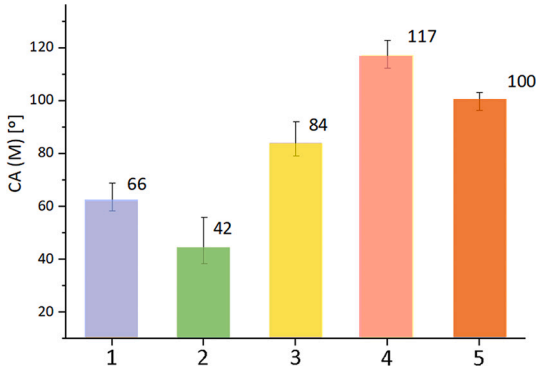

Fig. 4. Contact angle average values CA (M) and standard deviations obtained for the 1–5 hybrid samples.

properties on stone specimens.

3.3. Antimicrobial capacity

The antimicrobial test performed for 4 and 5 nano-enriched formulations against the bacteria *Arthrobacter spp.* demonstrated a bacterial inhibition effect in both cases (Fig. 5), thus, the NPs embedded into the hybrid matrix preserved their biocidal capability being also able to provide additional properties to CBDO-based hybrids. The n_w values detected for samples 4 and 5 were 0.25 and 0.31 mm, respectively. However, although cerium doping was employed to enhance self-cleaning and antimicrobial activity in the visible light range, the Petri dishes used did not allow the UV light fraction to pass and thus, the highest biocidal effect of Ce-doped TiO_2 NPs of sample 4 is expected to be obtained in outdoor conditions where UV radiation enables a complete photocatalytic effect [6,72,73].

3.4. Stone validation trials

Colorimetric measurements on the lithic samples revealed slight variations in lightness, hue and chroma values (L*, a* and b*) (Table S1) for the treatments based on the selected nano-enriched hybrid formulations, namely 4 and 5, which resulted in Delta E (ΔE) of 3.27 and 2.23, respectively, corresponding both to the *just noticeable* chromatic alteration level, according to the CIE*Lab Colour-Difference Thresholds classification [74]. Furthermore, by comparing colorimetric data obtained for non-treated samples with those collected on treated, after ageing experiments, it resulted that ΔE values were below 3.8, *i.e.* chromatic alterations below the *distinctively perceptible* level, thus confirming that exposure to an acidic atmosphere did not cause significant chromatic changes on the applied nano-enriched materials.

In order to evaluate the consolidating effect provided by the hybrid products to the stone samples, amplification images by the magnification glass were collected and SEM analysis were carried out (Figs. 6 and S3). The data evidenced how both coatings reduce the alveolization of the stone as well as the loss of cementing matrix during the accelerated ageing process.

These findings were further supported by the average mass loss values obtained from the ageing experiments. While untreated samples exhibited a mass loss of 1.1 %, stone samples treated with 4 and 5 formulations displayed values between 0.4 and 0.3 %, respectively. This outcome demonstrates the efficacy of both treatments as protective coatings, as they effectively reduced the stone matrix deterioration rate by a factor of three. Moreover, the Scotch test also revealed the same trend with a higher preservation of the stone surface integrity. This was evidenced by a reduction of 87 % and 92 % in the amount of disaggregated material during the peeling experiments, as a direct result of the treatment carried out before the ageing process.

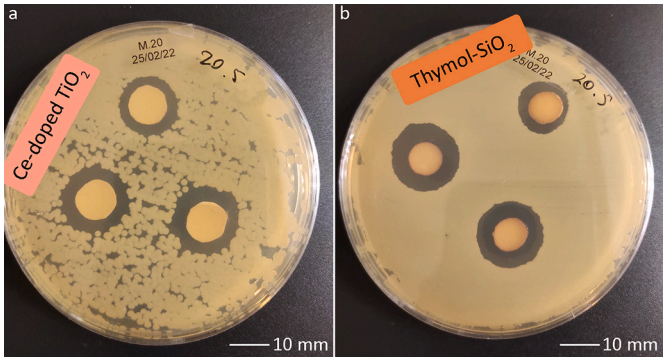

Fig. 5. Antimicrobial capacity against *Arthrobacter spp.* after 48 h of incubation, under visible light of the hybrids samples 4 and 5 doped with Ce-TiO_2 and thymol-SiO_2 NPs, respectively.

The whole set of results discussed in this study aligns with the properties of commercial products [50,52]. It highlights the superior capability of the coatings to prevent micro-cracks on the stone surface and demonstrates clear multifunctionality, including not only hydrophobic and consolidating properties, but also biocidal activity. Therefore, it is reasonable to conclude that the coatings enriched with NPs exhibited a significant capability to mitigate the mid-term decay, making them immediately effective in ensuring appropriate maintenance of the stone specimens and preventing further damages. Among the tested products, the thymol-loaded SiO_2 doped hybrid formulation showed the most significant multifunctional results overall.

4. Conclusions

A sustainable multifunctional bio-based epoxy-silica hybrid nanocomposite for stone conservation was successfully developed using a building block design approach by the combination of CBDO-DGE, GPTMS and OcTES enriched with thymol loaded into SiO_2 NPs. The resulting product exhibited excellent consolidating, flexibility and hydrophobic properties, as well as antimicrobial inhibition capacity. These appealing properties make it a highly promising multifunctional and eco-friendly option to upgrade the current commercial products available for preserving lithic materials against the most common deterioration patterns. Overall, the multianalytical approach employed in this study demonstrates the effectiveness of using renewable sources to design advanced materials with tailored properties through simultaneous synthetic strategies involving sol-gel processes and nanotechnology. In addition to its sustainability focus, the developed material is relatively easy to apply using standards tools, as the polymerization reaction can occur inside the stone (*i.e. in situ*). Consequently, after impregnation with low-density suspensions, a homogenous distribution throughout the porous network of the stone can be expected. Furthermore, this highly versatile bio-based hybrid nanocomposite can be easily scaled up to an industrial level. The synthesis protocol for obtaining the base resin involves a straightforward epoxidation process that utilizes a renewable source, which is abundantly available at a low cost. Moreover, during the material design phase, careful attention was paid to the commercial availability and affordability of the remaining required compounds. This approach ensures that the treatment is accessible to a wide range of professional users and makes it highly competitive compared to other commercial solutions, thanks to its exceptional multifunctional properties. However, further assessment is needed to evaluate its suitability along the time based on comprehensive fully stone durability tests, in accordance with UNE-EN, ASTM D and RILEM regulations, and other relevant standards.

CRediT authorship contribution statement

P. Irizar: Methodology, Formal analysis, Investigation, Writing – original draft, Data curation, Visualization. **A. Pintor-Rial:** Formal analysis. **I. Martinez-Arkarazo:** Resources, Writing – review & editing, Project administration, Funding acquisition. **M.A. Olazabal:** Project administration, Funding acquisition. **L. Ruiz-Rubio:** Investigation. **P. Cardiano:** Supervision, Visualization, Writing – review & editing. **O. Gomez-Laserna:** Conceptualization, Methodology, Formal analysis, Investigation, Resources, Writing – original draft, Writing – review & editing, Visualization, Funding acquisition, Project administration, Supervision.

Declaration of competing interest

The authors declare that they have no known competing financial interests or personal relationships that could have appeared to influence the work reported in this paper.

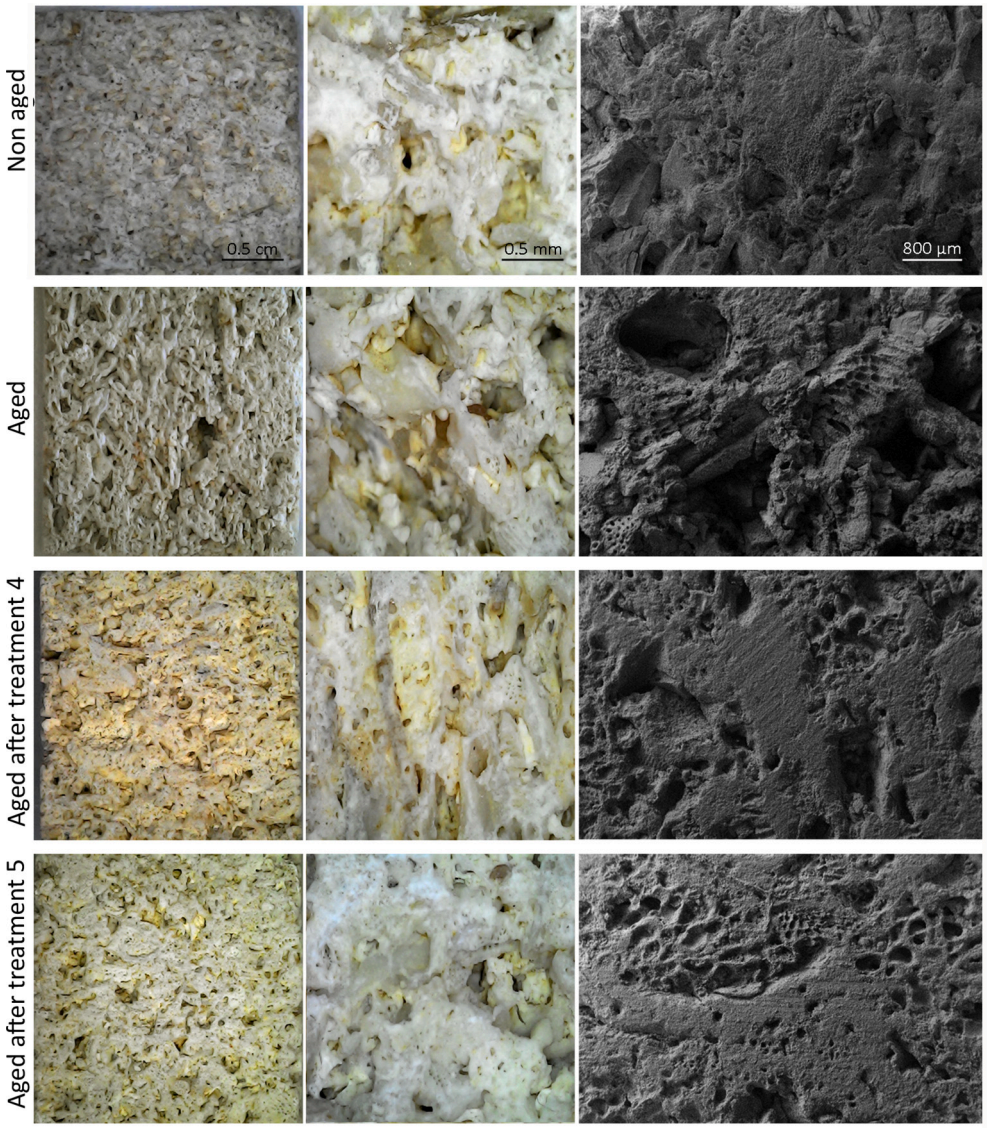

Fig. 6. Magnification photographs and SE images of the stone samples, untreated and treated, with the nano-enriched hybrid formulations 4 and 5, obtained from GPTMS and OCTES as silica precursors with Ce-TiO_2 and thymol-SiO_2 NPs, respectively, for the visual monitoring of their consolidating ability.

Data availability

Data will be made available on request.

Acknowledgements

This work has been financially supported by the projects PHETRUM (CTQ2017-82761-P) and DEMORA (PID2020-113391GB-I00) from the Spanish Ministry of Economy, Industry and Competitiveness (MINECO) and the Spanish Ministry of Science and Innovation (MICINN), respectively, as well as by the European Regional Development Fund (FEDER). The authors gratefully acknowledge Open Access funding provided by University of Basque Country. P. Irizar gratefully acknowledges his predoctoral grant from the MINECO (PRE2018-085888). The authors are grateful to the technical support provided by the Raman-LASPEA laboratory, the Nuclear Magnetic Resonance laboratory and to the Macrobehaviour, Mesostructure, Nanotechnology: Unit of Materials and Surfaces of The Advanced Research Facilities of the SGIker (UPV/EHU, MICINN, GV/EJ, ERDF and ESF).

Appendix A. Supplementary data

Supplementary data to this article can be found online at https://doi.org/10.1016/j.porgcoat.2023.107899.

References

[1] E.R.D. Fund, Built Cultural Heritage: Integrating Heritage Buildings into Contemporary Society, 2020.
[2] O. Gómez-Laserna, I. Arrizabalaga, N. Prieto-Taboada, M.Á. Olazabal, G. Arana, J. M. Madariaga, In situ DRIFT, Raman, and XRF implementation in a multianalytical methodology to diagnose the impact suffered by built heritage in urban atmospheres, Anal. Bioanal. Chem. 407 (2015) 5635–5647, https://doi.org/10.1007/s00216-015-8738-7.
[3] M. Sadat-Shojai, A. Ershad-Langroudi, Polymeric coatings for protection of historic monuments: opportunities and challenges, J. Appl. Polym. Sci. 112 (2009) 2535–2551, https://doi.org/10.1002/app.29801.
[4] P. Sanmartín, A. Rodríguez, U. Aguiar, Medium-term field evaluation of several widely used cleaning-restoration techniques applied to algal biofilm formed on a granite-built historical monument, Int. Biodeterior. Biodegradation 147 (2020), 104870, https://doi.org/10.1016/j.ibiod.2019.104870.
[5] European Union, Regulation (EU) No 528/2012 of the European Parliament and of the Council of 22 May 2012 Concerning the Making Available on the Market and Use of Biocidal Products, 2012.
[6] O. Gómez-Laserna, G. Lando, L. Kortazar, I. Martinez-Arkarazo, I. Monterrubio, E. Sevillano, P. Cardiano, M.Á. Olazabal, Eco-friendly nanocomposite products

based on BPA-free epoxy–silica hybrid materials for stone conservation, Archaeol. Anthropol. Sci. 11 (2019) 5799–5812, https://doi.org/10.1007/s12520-019-00904-6.
[7] O. Gómez-Laserna, P. Cardiano, M. Diez-Garcia, N. Prieto-Taboada, L. Kortazar, M.Á. Olazabal, J.M. Madariaga, Multi-analytical methodology to diagnose the environmental impact suffered by building materials in coastal areas, Environ. Sci. Pollut. Res. 25 (2018) 4371–4386, https://doi.org/10.1007/s11356-017-0798-0.
[8] S. Kumar, S.K. Samal, S. Mohanty, S.K. Nayak, Recent development of biobased epoxy resins: a review, Polym.-Plast. Technol. Eng. 57 (2018) 133–155, https://doi.org/10.1080/03602559.2016.1253742.
[9] E.A. Baroncini, S. Kumar Yadav, G.R. Palmese, J.F. Stanzione, Recent advances in bio-based epoxy resins and bio-based epoxy curing agents, J. Appl. Polym. Sci. 133 (2016) app.44103, https://doi.org/10.1002/app.44103.
[10] O. Gómez-Laserna, P. Irizar, G. Lando, L. Kortazar, A. Irto, L. Ruiz-Rubio, I. Martinez-Arkarazo, P. Cardiano, M.Á. Olazabal, Design of epoxy-silica hybrids based on cycloaliphatic diol of natural origin for conservation of lithic materials, Prog. Org. Coat. 151 (2021), 106028, https://doi.org/10.1016/j.porgcoat.2020.106028.
[11] P. Irizar, A. Irto, I. Martinez-Arkarazo, M.Á. Olazabal, P. Cardiano, O. Gomez-Laserna, Sugar-derived bio-based resins as platforms for the development of multifunctional hybrids with potential application for stone conservation, Mater. Today Commun. 31 (2022), 103662, https://doi.org/10.1016/j.mtcomm.2022.103662.
[12] S. Wang, Y. Qiu, Synthesis of SiO_2 nanoparticle epoxy resin composite and silicone-containing epoxy resin for coatings, Appl. Bionics Biomech. 2022 (2022) 1–10, https://doi.org/10.1155/2022/8227529.
[13] R. Striani, C. Esposito Corcione, G. Dell'Anna Muia, M. Frigione, Durability of a sunlight-curable organic–inorganic hybrid protective coating for porous stones in natural and artificial weathering conditions, Prog. Org. Coat. 101 (2016) 1–14, https://doi.org/10.1016/j.porgcoat.2016.07.018.
[14] P. Cardiano, Hydrophobic properties of new epoxy-silica hybrids, J. Appl. Polym. Sci. 108 (2008) 3380–3387, https://doi.org/10.1002/app.27985.
[15] P. Cardiano, S. Lo Schiavo, P. Piraino, Hydrorepellent properties of organic–inorganic hybrid materials, J. Non-Cryst. Solids 356 (2010) 917–926, https://doi.org/10.1016/j.jnoncrysol.2009.12.025.
[16] G.M.C. Gemelli, R. Zarzuela, F. Fernandez, M.J. Mosquera, Compatibility, effectiveness and susceptibility to degradation of alkoxysilane-based consolidation treatments on a carbonate stone, J. Build. Eng. 42 (2021), 102840, https://doi.org/10.1016/j.jobe.2021.102840.
[17] D. Schmidt, BISPHENOLA (BPA) FREE EPOXY RESINS, US 9,139,690 B2, 2015.
[18] N. Halawani, Ricardo K. Donato, H. Benes, J. Brus, L. Kobera, S. Pruvost, J. Duchet-Rumeau, J.-F. Gérard, S. Livi, Thermoset-thermoplastic-ionic liquid ternary hybrids as novel functional polymer materials, Polymer. 218 (2021), 123507, https://doi.org/10.1016/j.polymer.2021.123507.
[19] M. Adeel, B. Zhao, H. Mei, L. Li, S. Zheng, Nanostructured thermosets involving epoxy and poly(ionic liquid)-containing diblock copolymer, Polymer. 213 (2021), 123293, https://doi.org/10.1016/j.polymer.2020.123293.
[20] P.K. Balguri, D.G.H. Samuel, U. Thumu, A review on mechanical properties of epoxy nanocomposites, Mater. Today: Proc. 44 (2021) 346–355, https://doi.org/10.1016/j.matpr.2020.09.742.
[21] A. Shrivastava, Introduction to Plastics Engineering, William Andrew, Oxford, United Kingdom, Cambridge, MA, 2018.
[22] F. Gherardi, M. Roveri, S. Goidanich, L. Toniolo, Photocatalytic nanocomposites for the protection of European architectural heritage, Materials. 11 (2018) 65, https://doi.org/10.3390/ma11010065.
[23] N. Azadi, H. Parsimehr, A. Ershad-Langroudi, Cultural heritage protection via hybrid nanocomposite coating, Plast. Rubber Compos. 49 (2020) 414–424, https://doi.org/10.1080/14658011.2020.1784589.
[24] R.K. Donato, K.Z. Donato, H.S. Schrekker, L. Matějka, Tunable reinforcement of epoxy-silica nanocomposites with ionic liquids, J. Mater. Chem. 22 (2012) 9939, https://doi.org/10.1039/c2jm30830d.
[25] A. Kozirog, A. Wysocka-Robak, in: S. Handy (Ed.), Application of Ionic Liquids in Paper Properties and Preservation, Progress and Developments in Ionic Liquids, InTech, 2017, https://doi.org/10.5772/65860.
[26] K. Schmitz, S. Wagner, M. Reppke, C.L. Maier, E. Windeisen-Holzhauser, J.P. Benz, Preserving cultural heritage: analyzing the antifungal potential of ionic liquids tested in paper restoration, PLoS One 14 (2019), e0219650, https://doi.org/10.1371/journal.pone.0219650.
[27] A. El-Shamy, M. Abdel Bar, Ionic liquid as water soluble and potential inhibitor for corrosion and microbial corrosion for iron artifacts, Egypt. J. Chem. 0 (2021), https://doi.org/10.21608/ejchem.2021.43786.2887, 0–0.
[28] Q. Li, Y. Hu, B. Zhang, Phosphonium-based ionic liquids as antifungal agents for conservation of heritage sandstone, RSC Adv. 12 (2022) 1922–1931, https://doi.org/10.1039/D1RA09169G.
[29] L. Gontrani, Choline-amino acid ionic liquids: past and recent achievements about the structure and properties of these really "green" chemicals, Biophys. Rev. 10 (2018) 873–880, https://doi.org/10.1007/s12551-018-0420-9.
[30] A.M. Abdel-Karim, A.M. El-Shamy, A review on green corrosion inhibitors for protection of archeological metal artifacts, J. Bio- Tribo-Corros. 8 (2022) 35, https://doi.org/10.1007/s40735-022-00636-6.
[31] S. Eyssautier-Chuine, I. Franco-Castillo, A. Misra, J. Hubert, N. Vaillant-Gaveau, C. Streb, S.G. Mitchell, Evaluating the durability and performance of polyoxometalate-ionic liquid coatings on calcareous stones: preventing biocolonisation in outdoor environments, Sci. Total Environ. 884 (2023), 163739, https://doi.org/10.1016/j.scitotenv.2023.163739.
[32] A. Misra, I. Franco Castillo, D.P. Müller, C. González, S. Eyssautier-Chuine, A. Ziegler, J.M. de la Fuente, S.G. Mitchell, C. Streb, Polyoxometalate-ionic liquids (POM-ILs) as anticorrosion and antibacterial coatings for natural stones, Angew. Chem. Int. Ed. 57 (2018) 14926–14931, https://doi.org/10.1002/anie.201809893.
[33] V.V. Ermolaev, D.M. Arkhipova, V.A. Miluykov, A.P. Lyubina, S.K. Amerhanova, N. V. Kulik, A.D. Voloshina, V.P. Ananikov, Sterically hindered quaternary phosphonium salts (QPSs): antimicrobial activity and hemolytic and cytotoxic properties, IJMS. 23 (2021) 86, https://doi.org/10.3390/ijms23010086.
[34] Y. Xue, H. Xiao, Y. Zhang, Antimicrobial polymeric materials with quaternary ammonium and phosphonium salts, IJMS. 16 (2015) 3626–3655, https://doi.org/10.3390/ijms16023626.
[35] F. De Leo, P. Cardiano, G. De Carlo, S. Lo Schiavo, C. Urzì, Testing the antimicrobial properties of an upcoming "environmental-friendly" family of ionic liquids, J. Mol. Liq. 248 (2017) 81–85, https://doi.org/10.1016/j.molliq.2017.10.024.
[36] F. Antonelli, M. Bartolini, M.-L. Plissonnier, A. Esposito, G. Galotta, S. Ricci, B. Davidde Petriaggi, C. Pedone, A. Di Giovanni, S. Piazza, F. Guerrieri, M. Romagnoli, Essential oils as alternative biocides for the preservation of waterlogged archaeological wood, Microorganisms. 8 (2020), 2015, https://doi.org/10.3390/microorganisms8122015.
[37] M.R. Fidanza, G. Caneva, Natural biocides for the conservation of stone cultural heritage: a review, J. Cult. Herit. 38 (2019) 271–286, https://doi.org/10.1016/j.culher.2019.01.005.
[38] M. Spada, O.A. Cuzman, I. Tosini, M. Galeotti, F. Sorella, Essential oils mixtures as an eco-friendly biocidal solution for a marble statue restoration, Int. Biodeterior. Biodegradation 163 (2021), 105280, https://doi.org/10.1016/j.ibiod.2021.105280.
[39] F. Palla, M. Bruno, F. Mercurio, A. Tantillo, V. Rotolo, Essential oils as natural biocides in conservation of cultural heritage, Molecules. 25 (2020) 730, https://doi.org/10.3390/molecules25030730.
[40] H. Kim, S. Lee, B. Son, J. Jeon, D. Kim, Wonku Lee, H. Youn, J.-M. Lee, B. Youn, Biocidal effect of thymol and carvacrol on aquatic organisms: possible application in ballast water management systems, Mar. Pollut. Bull. 133 (2018) 734–740, https://doi.org/10.1016/j.marpolbul.2018.06.025.
[41] L. de Oliveira, K. Bouchmella, A. Picco, L. Capeletti, K. Gonçalves, J.H. dos Santos, J. Kobarg, M. Cardoso, Tailored silica nanoparticles surface to increase drug load and enhance bactericidal response, J. Braz. Chem. Soc. (2017), https://doi.org/10.21577/0103-5053.20170017.
[42] G. Cavallaro, G. Lazzara, S. Milioto, F. Parisi, Halloysite nanotubes for cleaning, consolidation and protection, Chem. Rec. 18 (2018) 940–949, https://doi.org/10.1002/tcr.201700099.
[43] M.E. David, R.-M. Ion, R.M. Grigorescu, L. Iancu, E.R. Andrei, Nanomaterials used in conservation and restoration of cultural heritage: an up-to-date overview, Materials. 13 (2020) 2064, https://doi.org/10.3390/ma13092064.
[44] N. Yan, Z. Zhu, J. Zhang, Z. Zhao, Q. Liu, Preparation and properties of ce-doped TiO2 photocatalyst, Mater. Res. Bull. 47 (2012) 1869–1873, https://doi.org/10.1016/j.materresbull.2012.04.077.
[45] A.P. Kanth, A.K. Soni, Application of nanocomposites for conservation of materials of cultural heritage, J. Cult. Herit. 59 (2023) 120–130, https://doi.org/10.1016/j.culher.2022.11.010.
[46] A. Rodrigues, B. Sena Da Fonseca, A.P. Ferreira Pinto, S. Piçarra, M.D.F. Montemor, TEOS nanocomposites for the consolidation of carbonate stone: the effect of nano-HAp and nano-SiO2 modifiers, Materials. 15 (2022) 981, https://doi.org/10.3390/ma15030981.
[47] F. Gherardi, P.N. Maravelaki, Advances in the application of nanomaterials for natural stone conservation, RILEM Tech. Lett. 7 (2022) 20–29, https://doi.org/10.21809/rilemtechlett.2022.159.
[48] M.B. Chobba, M.L. Weththimuni, M. Messaoud, D. Sacchi, J. Bouaziz, F. De Leo, C. Urzi, M. Licchelli, Multifunctional and durable coatings for stone protection based on Gd-doped nanocomposites, Sustainability. 13 (2021) 11033, https://doi.org/10.3390/su131911033.
[49] V. Renda, M.A. De Buergo, M.L. Saladino, E. Caponetti, Assessment of protection treatments for carbonatic stone using nanocomposite coatings, Prog. Org. Coat. 141 (2020), 105515, https://doi.org/10.1016/j.porgcoat.2019.105515.
[50] A. Zornoza-Indart, P. Lopez-Arce, N. Leal, J. Simão, K. Zoghlami, Consolidation of a Tunisian bioclastic calcarenite: from conventional ethyl silicate products to nanostructured and nanoparticle based consolidants, Constr. Build. Mater. 116 (2016) 188–202, https://doi.org/10.1016/j.conbuildmat.2016.04.114.
[51] G. Wang, Y. Chai, Y. Li, H. Luo, B. Zhang, J. Zhu, Sandstone protection by using nanocomposite coating of silica, Appl. Surf. Sci. 615 (2023), 156193, https://doi.org/10.1016/j.apsusc.2022.156193.
[52] A. Zornoza-Indart, P. Lopez-Arce, K. Zoghlami, N. Leal, J. Simão, Marine aerosol weathering of Mediterranean calcarenite stone: durability of ethyl silicate, nano Ca $(OH)_2$, nano SiO_2, and nanostructured consolidating products, Stud. Conserv. 64 (2019) 73–89, https://doi.org/10.1080/00393630.2018.1477654.
[53] U. Daood, J.P. Matinlinna, M.R. Pichika, K.-K. Mak, V. Nagendrababu, A.S. Fawzy, A quaternary ammonium silane antimicrobial triggers bacterial membrane and biofilm destruction, Sci. Rep. 10 (2020) 10970, https://doi.org/10.1038/s41598-020-67616-z.
[54] A. Cieniecka-Rosłonkiewicz, J. Pernak, J. Kubis-Feder, A. Ramani, A.J. Robertson, K.R. Seddon, Synthesis, anti-microbial activities and anti-electrostatic properties of phosphonium-based ionic liquids, Green Chem. 7 (2005) 855, https://doi.org/10.1039/b508499g.
[55] A. Escobar, M. Pérez, G. Romanelli, G. Blustein, Thymol bioactivity: a review focusing on practical applications, Arab. J. Chem. 13 (2020) 9243–9269, https://doi.org/10.1016/j.arabjc.2020.11.009.

[56] T.A. Nguyen, T.H. Nguyen, T.V. Nguyen, H. Thai, X. Shi, Effect of nanoparticles on the thermal and mechanical properties of epoxy coatings, J. Nanosci. Nanotechnol. 16 (2016) 9874–9881, https://doi.org/10.1166/jnn.2016.12162.
[57] A.W. Bauer, W.M.M. Kirby, J.C. Sherris, M. Turck, Antibiotic susceptibility testing by a standardized single disk method, Am. J. Clin. Pathol. 45 (1966) 493–496, https://doi.org/10.1093/ajcp/45.4_ts.493.
[58] M. Martí, B. Frígols, A. Serrano-Aroca, Antimicrobial characterization of advanced materials for bioengineering applications, JoVE (2018) 57710, https://doi.org/10.3791/57710.
[59] S. Rogalsky, J. Bardeau, L. Lyudmila, O. Tarasyuk, O. Bulko, O. Dzhuzha, T. Cherniavska, V. Kremenitsky, K. Larisa, S. Riabov, New promising antimicrobial material based on thermoplastic polyrethane modified with polymeric biocide polyhexamethylene guanidine hydrochloride, Mater. Chem. Phys. (2021) 124682, https://doi.org/10.1016/j.matchemphys.2021.124682.
[60] L.M. Gil-Martín, M.A. Fernández-Ruiz, E. Hernández-Montes, Mechanical characterization and creep behavior of a stone heritage material used in Granada (Spain): Santa Pudia Calcarenite, Rock Mech. Rock. Eng. 55 (2022) 5659–5669, https://doi.org/10.1007/s00603-022-02946-0.
[61] A. Calia, A.M. Mecchi, D. Colangiuli, L. Scudeler Baccelle, Conservation issues with calcarenites used as historical building materials in Syracuse (Southern Italy), QJEGH. 46 (2013) 485–492, https://doi.org/10.1144/qjegh2012-050.
[62] C. Jimenez-Lopez, F. Jroundi, C. Pascolini, C. Rodriguez-Navarro, G. Piñar-Larrubia, M. Rodriguez-Gallego, M.T. González-Muñoz, Consolidation of quarry calcarenite by calcium carbonate precipitation induced by bacteria activated among the microbiota inhabiting the stone, Int. Biodeterior. Biodegradation 62 (2008) 352–363, https://doi.org/10.1016/j.ibiod.2008.03.002.
[63] RILEM, Essais recommandés pour mesurer l'altération des pierres et évaluer l'efficacité des méthodes de traitement, Matériaux et Constructions 13, 1980 (n.d.) 275–252.
[64] M. Torabi-Kaveh, M. Moshrefyfar, S. Shirzaei, S.M.A. Moosavizadeh, B. Ménendez, S. Maleki, Application of resin-TiO_2 nanoparticle hybrid coatings on travertine stones to investigate their durability under artificial aging tests, Constr. Build. Mater. 322 (2022), 126511, https://doi.org/10.1016/j.conbuildmat.2022.126511.
[65] R.J. Flatt, F. Caruso, A.M.A. Sanchez, G.W. Scherer, Chemo-mechanics of salt damage in stone, Nat. Commun. 5 (2014) 4823, https://doi.org/10.1038/ncomms5823.
[66] M. Drdácký, J. Lesák, S. Rescic, Z. Slízková, P. Tiano, J. Valach, Standardization of peeling tests for assessing the cohesion and consolidation characteristics of historic stone surfaces, Mater. Struct. 45 (2012) 505–520, https://doi.org/10.1617/s11527-011-9778-x.
[67] NORMAL Protocol 43/93 (NORMAL 1993), (n.d.).
[68] D.R. T, The RRUFF project: an integrated study of the chemistry, crystallography, Raman and infrared spectroscopy of minerals, in: Program and Abstracts of the 19th General Meeting of the International Mineralogical Association in Kobe, Japan, 2006, 2006. https://cir.nii.ac.jp/crid/1571417124253896704. (Accessed 11 November 2022).
[69] P. Innocenzi, G. Brusatin, F. Babonneau, Competitive polymerization between organic and inorganic networks in hybrid materials, Chem. Mater. 12 (2000) 3726–3732, https://doi.org/10.1021/cm001139b.
[70] H. Maka, T. Spychaj, R. Pilawka, Epoxy resin/ionic liquid systems: the influence of imidazolium cation size and anion type on reactivity and thermomechanical properties, Ind. Eng. Chem. Res. 51 (2012) 5197–5206, https://doi.org/10.1021/ie202321j.
[71] K. Manoharan, Mohd.T. Anwar, S. Bhattacharya, Development of hydrophobic paper substrates using silane and sol–gel based processes and deriving the best coating technique using machine learning strategies, Sci. Rep. 11 (2021) 11352, https://doi.org/10.1038/s41598-021-90855-7.
[72] Y. Ren, Y. Han, Z. Li, X. Liu, S. Zhu, Y. Liang, K.W.K. Yeung, S. Wu, Ce and Er Co-doped TiO2 for rapid bacteria- killing using visible light, Bioact. Mater. 5 (2020) 201–209, https://doi.org/10.1016/j.bioactmat.2020.02.005.
[73] E. Cerrato, E. Gaggero, P. Calza, M.C. Paganini, The role of cerium, europium and erbium doped TiO2 photocatalysts in water treatment: a mini-review, Chem. Eng. J. Adv. 10 (2022), 100268, https://doi.org/10.1016/j.ceja.2022.100268.
[74] K. Bieske, C. Vandahl, A Study About Colour Difference Thresholds, in: Ilmenau, Deutschland, 2007.